GIS-based weights-of-evidence modelling of rainfall-induced landslides in small catchments for landslide suscept...

Biswajeet Pradhan

Environmental ...

Environ Geol (2008) 54:311–324
DOI 10.1007/s00254-007-0818-3

ORIGINAL ARTICLE

GIS-based weights-of-evidence modelling of rainfall-induced landslides in small catchments for landslide susceptibility mapping

Ranjan Kumar Dahal · Shuichi Hasegawa · Atsuko Nonomura · Minoru Yamanaka · Takuro Masuda · Katsuhiro Nishino

Received: 2 February 2007 / Accepted: 15 May 2007 / Published online: 12 June 2007

Abstract Landslide susceptibility mapping is a vital tool for disaster management and planning development activities in mountainous terrains of tropical and subtropical environments. In this paper, the weights-of-evidence modelling was applied, within a geographical information system (GIS), to derive landslide susceptibility map of two small catchments of Shikoku, Japan. The objective of this paper is to evaluate the importance of weights-of-evidence modelling in the generation of landslide susceptibility maps in relatively small catchments having an area less than 4 sq km. For the study area in Moriyuki and Monnyu catchments, northeast Shikoku Island in west Japan, a data set was generated at scale 1:5,000. Relevant thematic maps representing various factors (e.g. slope, aspect, relief, flow accumulation, soil depth, soil type, land use and distance to road) that are related to landslide activity were generated using field data and GIS techniques. Both catchments have homogeneous geology and only consist of Cretaceous granitic rock. Thus, bedrock geology was not considered in data layering during GIS analysis. Success rates were also estimated to evaluate the accuracy of landslide susceptibility maps and the weights-of-evidence modelling was found useful in landslide susceptibility mapping of small catchments.

Keywords Landslide · GIS · Weights-of-evidence modelling · Susceptibility map · Rainfall

R. K. Dahal · S. Hasegawa · A. Nonomura · M. Yamanaka · T. Masuda
Department of Safety Systems Construction Engineering, Faculty of Engineering, Kagawa University, 2217-20, Hayashi-cho, Takamatsu City 761-0396, Japan

R. K. Dahal (✉)
Department of Geology, Tri-Chandra Multiple Campus, Tribhuvan University, Ghantaghar, Kathmandu, Nepal
e-mail: ranjan@ranjan.net.np
URL: http://www.ranjan.net.np

K. Nishino
OYO Corporation, 2-61-5, Toro-Cho, Kita-Ku, Saitama 331-8688, Japan

Introduction

Landslides are amongst the most damaging natural hazards in the mountainous terrain of tropical and subtropical environments. Potential sites that are particularly prone to landslides should therefore be identified in advance so as to reduce disaster damages. Landslide hazard assessment can be a vital tool to understand the basic characteristics of the terrains that are prone to failure, especially during extreme climatic events. According to Varnes (1984), the landslide hazard can be assessed in terms of probability of occurrence of a potentially damaging landslide phenomenon within a specified period of time and within a given area. Moreover, intrinsic and extrinsic variables are used to determine the landslide hazard in an area (Siddle 1991; Wu and Siddle 1995; Atkinson and Massari 1998; Dai et al. 2001; Çevik and Topal 2003). The intrinsic variables determine the susceptibility of landslides and include bedrock geology, geomorphology, soil depth, soil type, slope gradient, slope aspect, slope convexity and concavity, elevation, engineering properties of the slope material, land use pattern, drainage patterns and so on. Similarly, the extrinsic variables tend to trigger landslides in an area of given susceptibility and may include heavy rainfall, earthquakes and volcanoes. Observations and experiences show that the probability of landslide occurrence depends on both intrinsic and extrinsic variables. However, the

extrinsic variables are site specific and possess temporal distribution. Moreover, they are difficult to be estimated because of lack of information about the spatial distribution. Hence, in landslide hazard assessment practice, the term ''landslide susceptibility mapping'' is addressed without considering the extrinsic variables in determining the probability of occurrence of a landslide event (Dai et al. 2001).

Most published literatures on landslide hazard mapping mainly deal with landslide susceptibility mapping. There are numerous studies involving landslide hazard evaluation, and particularly, Guzzetti et al. (1999) have summarised many cases of landslide hazard evaluation studies. Landslide susceptibility may also be assessed through heuristic, deterministic and statistical approaches (Okimura and Kawatani 1986; Yin and Yan 1988; Van Westen and Bonilla 1990; Soeters and Van Westen 1996; Van Westen and Terlien 1996; Gökceoglu and Aksoy 1996; Pachauri et al. 1992; Van Westen 2000; Lee and Min 2001; Dai et al. 2001; Zêzere et al. 2004; Van Westen et al. 2003; Saha et al. 2005). Heuristic approach is a direct or semi direct mapping methodology, in which a direct relationship is established between the occurrence of slope failures and the causative terrain parameters during the landslide inventory. Therefore, in this approach, the opinions of the experts are very important to estimate landslide potential from the data involving intrinsic variables. Similarly, assigning weight values and ratings to the variables is very subjective and the results are not reproducible. Deterministic approaches, however, are based on slope stability analyses and are only applicable when the ground conditions are relatively homogeneous across the study area and the landslide types are known. Mainly, the infinite slope stability model has been widely used to assess landslide susceptibility in deterministic approaches (Wu and Sidle 1995; Terlien 1996; Gökceoglu and Aksoy 1996), and such a stability model needs a high degree of simplification of the intrinsic variables. Statistical approach, on the other hand, is an indirect susceptibility mapping methodology, which involves statistical determination of the combinations of variables that have led to landslide occurrence in the past. All possible intrinsic variables are entered into a GIS and crossed for their analysis with a landslide inventory map. Both simple or bivariate and multivariate statistical approaches have been used widely in such a statistical approach of landslide susceptibility mapping (Siddle et al. 1991; Atkinson and Massari 1998; Van Westen 2000; Dai et al. 2001).

In the past, susceptibility assessment and mapping were considered to be laborious and time-consuming jobs, but at present they are comparatively easy due to significant developments in computer applications and geographical information systems (GIS). Keeping this in mind, in this study, landslide susceptibility was evaluated by GIS technique using the weights-of-evidence modelling with respect to the bivariate statistical approach. The study area was selected in the northeastern part of Shikoku Island in west Japan that suffered extensive landslide damage during the heavy typhoon rainfall of 2004 and which is a suitable case for the evaluation of the frequency and distribution of rainfall-induced landslides for susceptibility mapping.

The study area

Shikoku is the smallest of the four main islands of Japan (total area 18,800 km^2), situated south of the island of Honshu and east of the island of Kyushu, between Seto Inland Sea and the Pacific Ocean. It is 225 km long and 50–150 km wide with more than 80% of land consisting of steep mountain slopes. It has few plain areas along the coastal lines and elevated peaks in the central part. The mountains are almost covered by thick forests of subtropical broad-leaved trees, Japanese cedars and Japanese bamboos. The mean annual precipitation of Shikoku ranges from 3,500 to 1,000 mm. Due to the geological and morphological settings, landslides and floods caused by typhoon rainfall are very frequent in Shikoku (Hiura et al. 2005; Dahal et al. 2006).

Although the climate of the northern part of Shikoku Island is an inland-type climate, like the Mediterranean region, and subsequently has less rainfall (annual rainfall 1,000 mm only), the area occasionally suffers from extreme typhoon-brought rainfall, which sometimes exceeds 750 mm in 1 day. In 2004, Shikoku experienced extreme events of typhoon rainfall and faced huge losses of life and property. Kagawa, the northeastern prefecture of Shikoku, was hit by four typhoons (0415, 0416, 0421 and 0423) in 2004 and suffered loss of lives and property because of the many landslides triggered by the typhoon rainfall. Among these disaster events, small river catchments, Moriyuki and Monnyu, situated in the eastern part of the Kagawa prefecture (Fig. 1), were confronted by typhoon 0423 (Tokage) and suffered extensive damages. From 19 October through 20 October 2004, typhoon 0423 produced 674 and 495 mm of rain in a 48 h period on Moriyuki and Monnyu of eastern Kagawa, respectively. On 20 October, a rain-gauge station in the Kusaka pass (located within 1 km aerial distance from Moriyuki catchment) recorded 582 mm of rain in 24 h with a maximum 116 mm/h rainfall intensity. Likewise, Monnyu area has a rain gauge station close to the failure sites. In this station, on 20 October, 412 mm of rain was recorded in 24 h with a maximum 76 mm/h rainfall intensity (Fig. 2). These are the highest precipitations of those areas in the last 30 years.

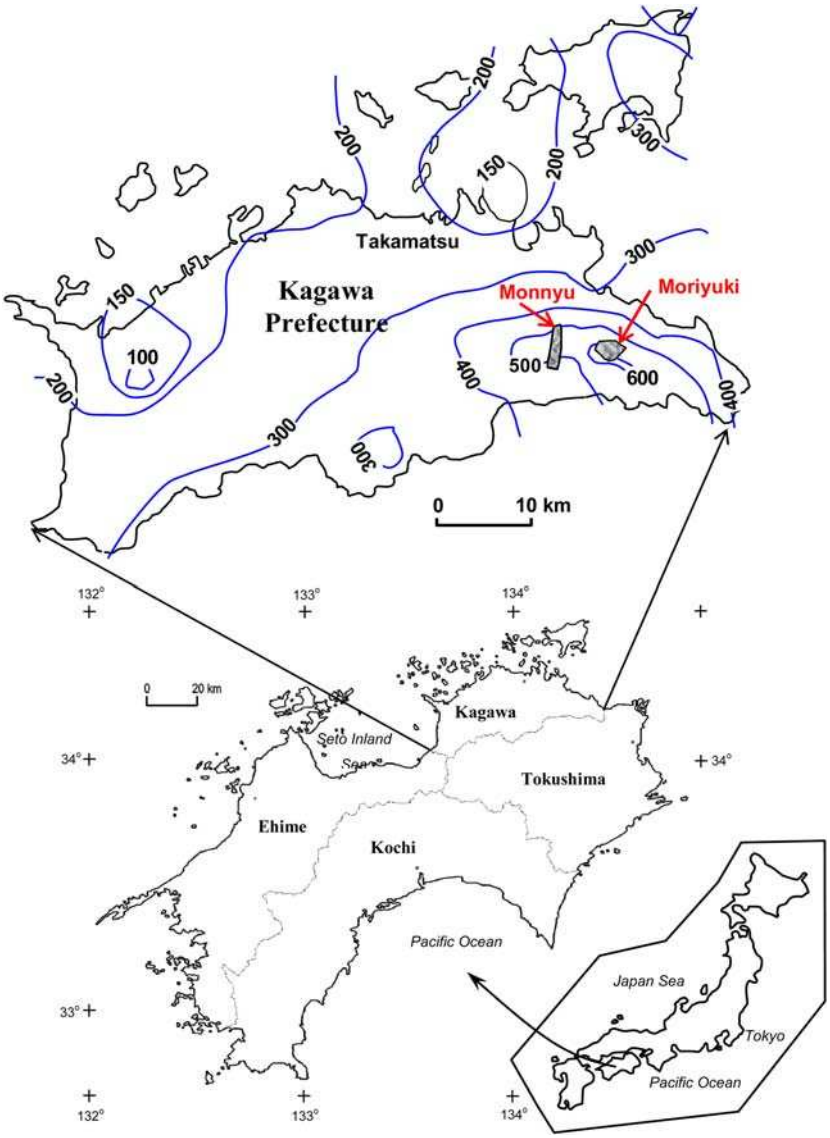

Fig. 1 Location of Moriyuki and Monnyu in northeast Shikoku, Japan and rainfall isohyetal map during typhoon 0423 (October 19 and 20, 2004)

These rainfall events triggered more than 300 landslides in Moriyuki and Monnyu catchment areas and debris flows occurred. Therefore, these two small catchments, Moriyuki and Monnyu, were selected for this study.

Geologically, the study area lies in the Ryoke Belt (Hasegawa and Saito 1991) of Shikoku. This belt is composed of late Cretaceous granitic rocks, late Cretaceous sedimentary rocks (Izumi Group) and Miocene volcanic rocks (Sanuki Group). Particularly, the Moriyuki and Monnyu catchments are situated on a zone of Cretaceous granitic rocks (Saito et al. 1972).

Weights-of-evidence modelling

In this study, the weights-of-evidence modelling was used for the large-scale landslide susceptibility mapping. It uses the Bayesian probability model and was originally developed for mineral potential assessment (Bonham-Carter et al. 1988, 1989; Agterberg et al. 1993; Bonham-Carter 1994). Several authors have applied the weights-of-evidence method to mineral potential mapping using the GIS in many countries (Emmanuel et al. 2000; Harris et al. 2000; Carranza and Hale 2002; Tangestani and Moore 2001). Cheng (2004) used this method for locating flowing wells and Daneshfar and Benn (2002) used it to understand spatial associations between faults and seismicity. Zahiri et al. (2006) used it for mapping of cliff instabilities associated with mine subsidence. This method has been started to apply to landslide susceptibility mapping also (Lee et al. 2002; Van Westen et al. 2003, Lee and Choi 2004, Lee 2004, Lee and Talib 2005, Lee and Sambath 2006). This method is simple, easy to use and less time consuming (Soeters and Van Westen 1996; Süzen and

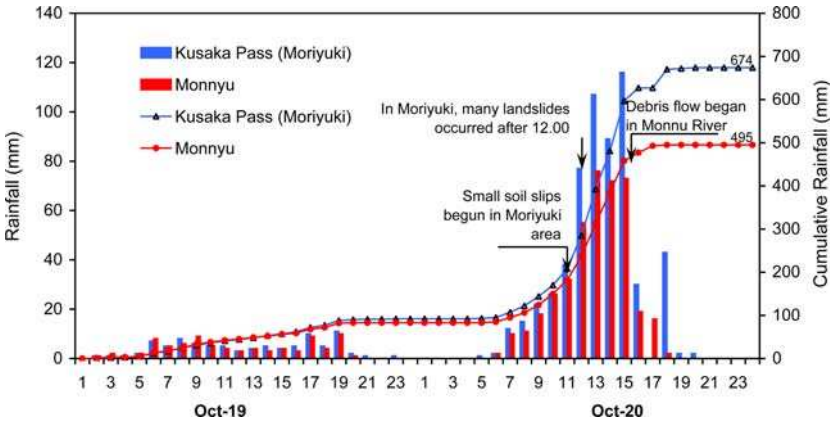

Fig. 2 Rainfall pattern and time of failures in Moriyuki and Monnyu during typhoon 0423

Doyuran 2004) and it can be performed rather easily with most GIS software packages.

A detailed description of the mathematical formulation of the method is available in Bonham-Carter (1994) and Bonham-Carter et al. (1989). The method calculates the weight for each landslide predictive factor (B) based on the presence or absence of the landslides (L) within the area, as indicated in Bonham-Carter et al. (1994) as follows:

$$W_i^+ = \ln \frac{P\{B|L\}}{P\{B|\bar{L}\}} \quad (1)$$

$$W_i^- = \ln \frac{P\{\bar{B}|L\}}{P\{\bar{B}|\bar{L}\}} \quad (2)$$

where P is the probability and ln is the natural log. Similarly, B is the presence of potential landslide predictive factor, $\bar{B}$ is the absence of a potential landslide predictive factor, L is the presence of landslide and $\bar{L}$ is the absence of a landslide. A positive weight (W_i^+) indicates that the predictable variable is present at the landslide locations and the magnitude of this weight is an indication of the positive correlation between the presence of the predictable variable and the landslides. A negative weight (W_i^-) indicates the absence of the predictable variable and shows the level of negative correlation. The difference between the two weights is known as the weight contrast, W_f ($W_f = W_i^+ - W_i^-$); the magnitude of the contrast reflects the overall spatial association between the predictable variable and the landslides.

Although weights-of-evidence modelling has not been previously applied in landslide susceptibility mapping of small catchments, the suitability of the technique for this purpose is evident in its successful use in other studies for examining susceptibility, spatial relationships and the distribution of particular features. The catchments selected for modelling have typical spatial and physical characters. Both selected catchments have an area less than 4 sq km. Both consist of landslides triggered by rainfall and the intrinsic variables are easily quantifiable in the field, and the production of accurate landslide conditioning factor maps is feasible. The two catchments are situated in the same climatic condition. Moreover, they have similar bedrock geology, same type of land use pattern, similar engineering properties of soil and they were affected by the same typhoon Tokage at the same time and on the same day. Considering all these typical characters, the main objectives of this study are listed as follows.

- To assess the types of landslides and landslide controlling factors on the northeastern terrain of Shikoku Island on a small catchment basis.
- To establish the weights of intrinsic variables causing landslides in one area (Moriyuki) and to apply the same methodology for establishing weights of similar type of intrinsic variables in the other area (Monnyu).
- To validate the weights-of-evidence modelling in the two catchments having similar intrinsic variables causing landslides triggered by the same extrinsic variable (typhoon rainfall).
- To test the reliability of weights-of-evidence model for the small catchments that have many similar spatial and physical characters.

Data acquisition

For the landslide susceptibility mapping, the main steps were data collection and construction of spatial database from which relevant factors were extracted, followed by assessment of the landslide susceptibility using the relationship between landslide and landslide predictive factors, and validation of results. A key approach to this method is that the occurrence possibility of landslide will be comparable with observed landslides.

In the initial stage of this study, for each area, a number of thematic data of predictive factors were identified, viz slope, slope aspect, geology, soil type, soil depth, land use,

distance to road, etc. Topographic maps, colour aerial photographs taken by Kagawa Prefecture Office immediately after the disaster events of 2004 and geological maps of northeast Kagawa prepared by Saito et al. (1972) were considered as basic data sources to generate these layers. Field surveys were also carried out for data collection and to prepare data layers of various factors, as well as to verify the geological map prepared by Saito et al. (1972). A landslide distribution map was also prepared on field. These data sources were used to generate various data layers using GIS software ILWIS 3.3. Brief descriptions of each data layer preparation procedure are given here.

Landslide characteristics and inventory maps

A landslide inventory map is the simplest output of direct landslide mapping. It shows the location of discernible landslides. It is a key factor used in landslide susceptibility mapping by weights-of-evidence modelling because overlay analysis requires an inventory map. In the Moriyuki catchment, 201 landslides were detected, and in the Monnyu catchment, 142 landslides were mapped. Landslide inventory maps were prepared on field and later the boundary of landslide was again refined with the help of aerial photographs of 1:5,000 scale. There were mainly translational and flow types of landslides in both catchments. Both types of failures were mapped out during inventory mapping.

A data sheet was also used to collect information of representative landslides in the study area. A total of 76 landslides of the Moriyuki and 40 landslides of the Monnyu area were visited on field for analysis of the nature of slides (length, height, depth, classification, etc.) and the data sheet was filled for each slide. These landslides were selected on the basis of the following considerations:

- Variations in landslide size, depth and relative location with respect to slope face and slope morphology (concave, convex and planar) among the total sites.
- Variations in slope orientation, slope height, slope angle, extent of vegetation and thickness of failure.
- Accessibility of slope with respect to investigations and measurements.

From the field study, it was found that the depth of failure was <2 m in more than 70% of slides and more than 70% of slides had a length of <10 m. Study of volume of failed materials revealed that 95% of landslides had a volume of less than 1000 m^3, whereas in Moriyuki all landslides had a volume of less than 1000 m^3. Likewise, more than 60% of failure occurred within residual soil and at the contact of bedrock and residual soil. About 20% of failures were found in fractured bedrocks and few (about 10%) failures were found at the contact between bedrock and colluvium and within the colluvium. This detailed study of selected landslides assists in quantifying the overall landslides scenario of the area and also suggests most representative classes for thematic data in GIS analysis.

Landslide inventory maps of both catchments were prepared in GIS, in which, only landslide scars (main failure portion) were used to delineate the landslides. The raster landslide inventory maps of both the areas are given in Fig. 3.

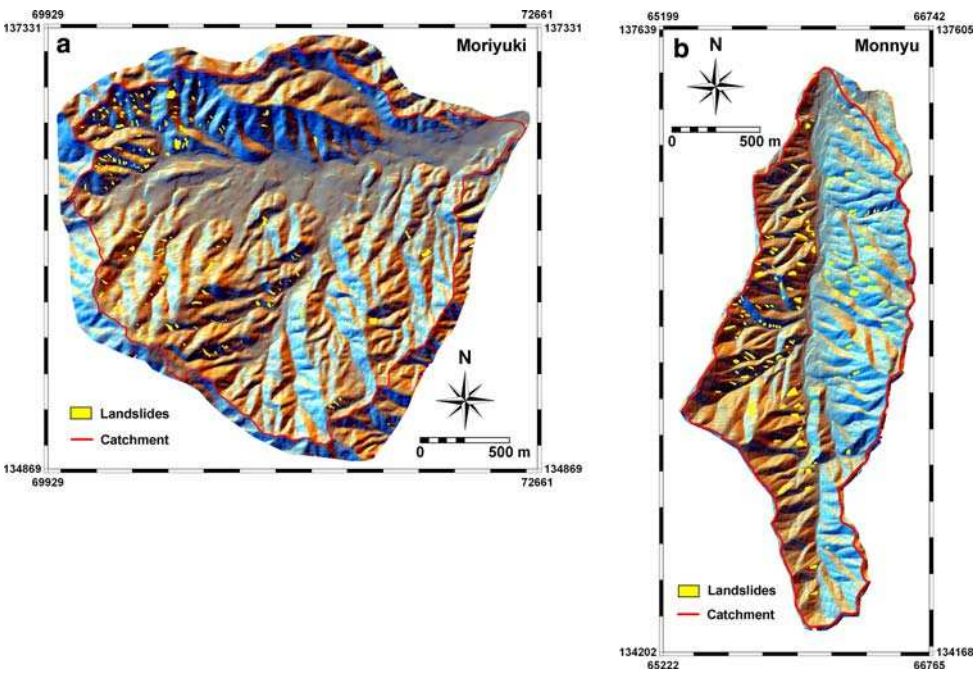

Fig. 3 Landslide inventory maps of the Moriyuki and Monnyu catchments

Geological maps

Geology plays an important role in landslide susceptibility studies because different geological units have different susceptibilities to active geomorphological processes (Anbalagan 1992; Pachauri et al. 1998; Dai et al. 2001, Lee and Talib 2005). As mentioned in the earlier section, cretaceous granite is the main rock unit of Moriyuki and Monnyu catchments as per the geological map (1:50,000 scale) prepared by Saito et al. (1972). During a field visit, rock exposures were also investigated specially in terms of mineralogical assemblages. Some thin section slides were also prepared to study minerals under a petrological microscope. Mineralogical study confirmed that Cretaceous granitic units in the Moriyuki area consist of biotite-granite in the northern part, whereas the southern part has slight granodioritic affinity. Similarly, in Monnyu, granodiorite is noticed in almost the whole area, except for a few areas of the northern part that has little affinity for biotite-granite. Few basaltic veins were also noticed in both catchments. Field studies as well as the study of existing geological maps and petrological study in the lab could not help to identify the spatial distribution of biotite-granite and granodiorite. Thus, it was considered that both catchments have monotonous rock units and geology was not needed to be considererd as a potential landslide predictive factor during weights-of-evidence modelling.

Digital elevation model -based derivatives

A digital elevation model (DEM) representing the terrain is a key to generate various topographic parameters, which influence the landslide activity in an area. Hence, DEM was prepared by digitising contours of 5 m interval in Moriyuki and 2 m interval in Monnyu from the topographic map of scale 1:5,000. The digitised contours were interpolated and resampled to 2.5×2.5 m^2 pixel size. From this DEM, thematic data layers like slope, aspect and relative relief were prepared. Slope data layer, an important parameter in slope stability considerations, comprises of eight classes. This classification was decided after measuring the slope angle of the failed slope during landslide inventory mapping. Field measurement of a total of 76 landslides of Moriyuki and 40 landslides of Monnyu catchments signified that most of the landslides occurred at slope angles between 26° and 51°. Thus, a total of seven classes, >10°, 10°–20°, 20°–30°, 30°–40°, 40° –50°, 50°–60°, >60°, were used to prepare the slope map. Aspect is referred to as the direction of maximum slope of the terrain surface. For the selected catchments, it is divided into nine classes, namely, N, NE, E, SE, S, SW, W, NW and flat. Relative relief data layer was prepared from the difference in maximum and minimum elevation and is sliced into eleven classes at 50 m elevation difference.

Land use

Land use is also one of the key factors responsible for the occurrence of landslides, since, barren slopes are more prone to landslides. In contrast, vegetative areas tend to reduce the action of climatic agents such as rain, etc., thereby preventing the erosion due to the natural anchorage provided by the tree roots and, thus, are less prone to landslides (Gray and Leiser 1982; Styczen and Morgan 1995; Greenway 1987). Based on the aerial photographs taken 10 days after the disaster events of 2004 and the field visit, nine land use classes that may have an impact on landslide activity in the region have been considered. These classes are dense forest, sparse forest, shrubs, bare with sparse shrubs, grassland, agriculture, irrigation pond, riverbed and settlement. The land use data layer was generated as vector polygons and they were converted to raster land use map by employing rasterise operation in ILWIS 3.3.

Distance to road

One of the controlling factors for the stability of slopes is road construction activity. This factor map was generated as per the hypothesis that landslides may be more frequent along roads, due to inappropriate cut slopes and drainage from the road. In order to produce the map showing the distance to roads, the road segment map was rasterised and the distance to these roads calculated in metres. The resultant map was then sliced to give a raster map showing the distance to roads divided into seven classes. The seven classes are 0–10, 10–20, 20–30, 30–50, 50–100, 100–200 and >200 m. For both catchments, the same classification scheme was used.

Flow accumulation

Following rainfall events, water flows from areas of convex curvature and accumulates in areas of concave curvature. This process is known as flow accumulation and is usually remarkable at the upstream segment of the catchment. Flow accumulation is a measure of the land area that contributes surface water to an area where surface water can accumulate. This parameter was considered as relevant to this study, because it defines the locations of water concentration after rainfall and those locations are likely to have a high landslide incidence. Flow accumulation can be explained as the number of pixels, or area, which contributes to runoff of a particular pixel. Flow accumulation measures the area of a watershed that contributes runoff to

the pixel. In fact, flow accumulation is also a DEM-based derivative and the DEM hydro-processing operation in ILWIS 3.3 calculates the flow accumulation of a watershed. The flow accumulation operation performs a cumulative count of the number of pixels that naturally drain into outlets.

For both Moriyuki and Monnyu catchments, the flow accumulation maps were prepared and classified into eight classes using histogram information and calculated cumulative percentages. In both catchments, about 50% of area has 3–20 cells contributing to their flow and main drainage.

Soil depth

During field study, detailed soil mapping were carried out in order to prepare the soil depth map of both catchments. Landslides mapping as per the prescribed data sheet help to categorise the most susceptible soil depth in both catchments. From the study of selected landslides, it is noticed that mainly soil depth of 0.5–2 m has maximum susceptibility to failure. There are some failures in zones having a 2–3.5 m soil depth also. Thus, three soil depth classes, <2, 2–4 and >4 m, were established to create a thematic layer of soil depth.

Soil type

Soils of the study area were geologically classified and soil maps were prepared for both catchments. Three categories, alluvial soil, colluvial soil and residual soil deposits, were identified on field as per the genesis.

Thus, finally a total of eight factors maps (slope, aspect, relief, flow accumulation, soil depth, soil type, land use and distance to road) were selected as thematic data for analysis. The all factor maps prepared in GIS for both Moriyuki and Monnyu are given in Figs. 4 and 5, respectively. Analysis procedures and results are discussed in the following sections.

Analysis and result

To evaluate the contribution of each factor towards landslide hazard, the existing landslide distribution data layer was compared to various thematic data layers separately. For this purpose, Eqs. (1) and (2) were written in a number of pixel format as follows.

$$W_i^+ = \ln \frac{\frac{N\text{pix}_1}{N\text{pix}_1+N\text{pix}_2}}{\frac{N\text{pix}_3}{N\text{pix}_3+N\text{pix}_4}} \quad (3)$$

$$W_i^- = \ln \frac{\frac{N\text{pix}_2}{N\text{pix}_1+N\text{pix}_2}}{\frac{N\text{pix}_4}{N\text{pix}_3+N\text{pix}_4}} \quad (4)$$

where $N\text{pix}_1$ is the number of pixels representing the presence of both potential landslide predictive factor and landslides, $N\text{pix}_2$ is the number of pixels representing the presence of landslides and absence of potential landslide predictive factor, $N\text{pix}_3$ is the number of pixels representing the presence of potential landslide predictive factor and absence of landslides, $N\text{pix}_4$ is the number of pixels representing the absence of both potential landslide predictive factor and landslides

All thematic maps were stored in raster format (985 rows and 1,093 columns for the Moriyuki catchment and 1,390 rows and 628 columns for the Monnyu catchment) with a pixel size of 2.5 m. The factor maps were all combined with the landslide inventory map for the calculation of the positive and negative weights. The calculation procedure was written in the form of a script file in ILWIS 3.3, consisting of a series of GIS commands to support Eqs. (3) and (4). Since all of the maps are multi-class maps, containing several classes, the presence of one factor, such as dense forest implies the absence of the other factors of the same land use map. Therefore in order to obtain the final weight of each factor, the positive weight of the factor itself was added to the negative weight of the other factors in the same map (Van Westen et al. 2003). The final calculated weights for both catchments are given in Table 1.

The resulting total weights, as shown in Table 1, directly indicate the importance of each factor. If the total weight is positive, the factor is favourable for the occurrence of landslides; if it is negative, it is not. It also can be concluded from Table 1 that some of the factors show hardly any relation with the occurrence of landslides, as evidenced by weights close to 0. For example, distance from roads classes of both catchments show values that oscillate around zero, without any extreme positive or negative values. This indicates that distance from roads is not a very sensitive predicting factor in both catchments. The frequency ratio (%landslide/%area) assists in assessing the relationship between the factors and landslide occurrences (Lee and Sambath 2006). For example, the slope aspect southeast shows high probability of landslide occurrences in Moriyuki, whereas south slope is more vulnerable in Monnyu.

The weights are assigned to the classes of each thematic layers, respectively, to produce weighted thematic maps, which were overlaid and numerically added according to Eq. (5) to produce a landslide susceptibility index (LSI) map.

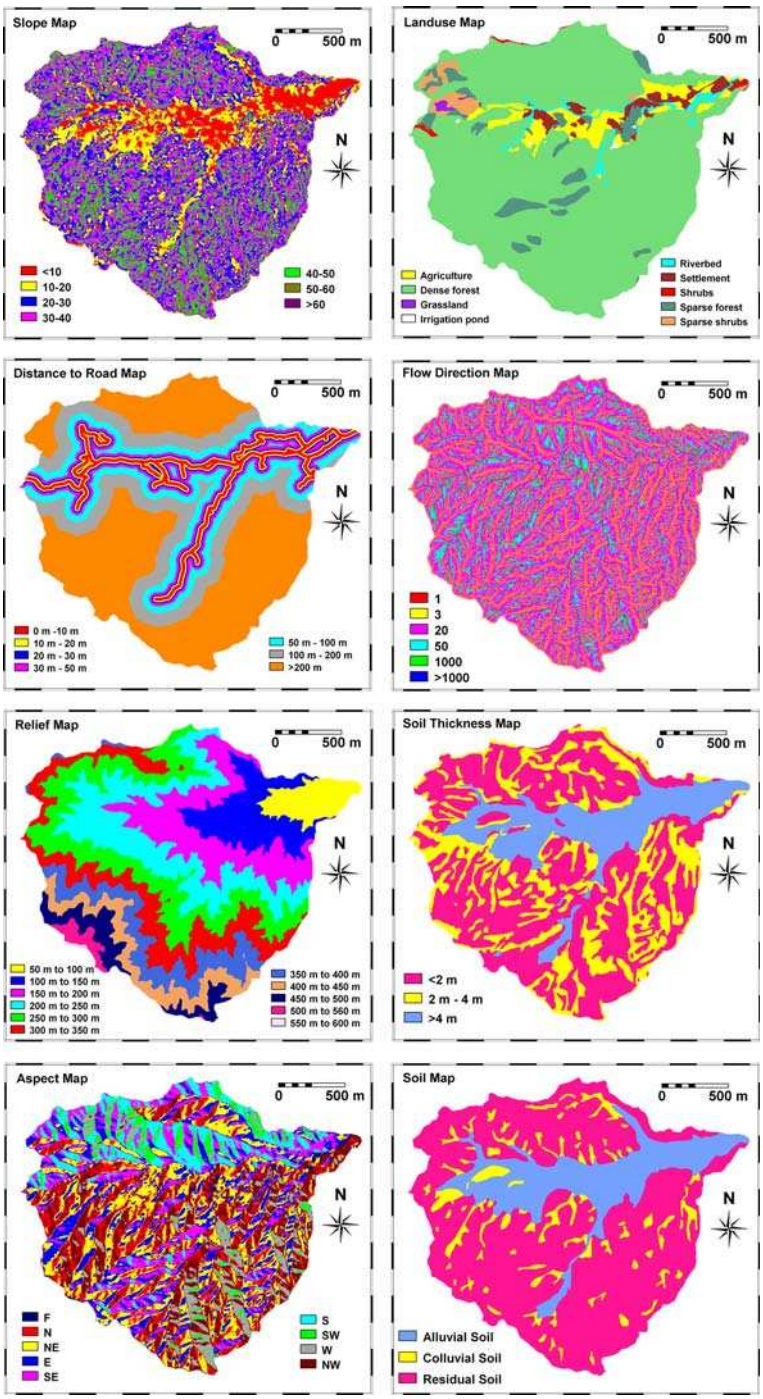

Fig. 4 Various thematic data layers prepared in GIS for the Moriyuki area

$$(\mathrm{LSI} = W_f\mathrm{Slope} + W_f\mathrm{Aspcls} + W_f\mathrm{Relief} + W_f\mathrm{FA} + W_f\mathrm{Soil} + W_f\mathrm{Depth} + W_f\mathrm{Landuse} + W_f\mathrm{Roadis}) \quad (5)$$

where W_fSlope, W_fAspcls, W_fRelief, W_fFA, W_fSoil, W_fDepth, W_fLanduse and W_fRoadis are distribution-derived weight of slope, slope aspect, relief, flow accumulation, soil type, soil depth, landuse and distance to road factor maps, respectively. Thus, two attribute maps of Moriyuki and Monnyu catchments were prepared from the respective LSI values. The LSI values are found to lie in the range of –22.820 to 7.224 for Moriyuki and –20.589 to 5.402 for Monnyu.

The capability of LSI values to predict landslide occurrences was verified with the help of the success rate (Chung and Fabbri 1999) curve and effect analysis (Lee 2004; Lee and Talib 2005; Lee and Sambath 2006). The success rate indicates how much percentage of all land-

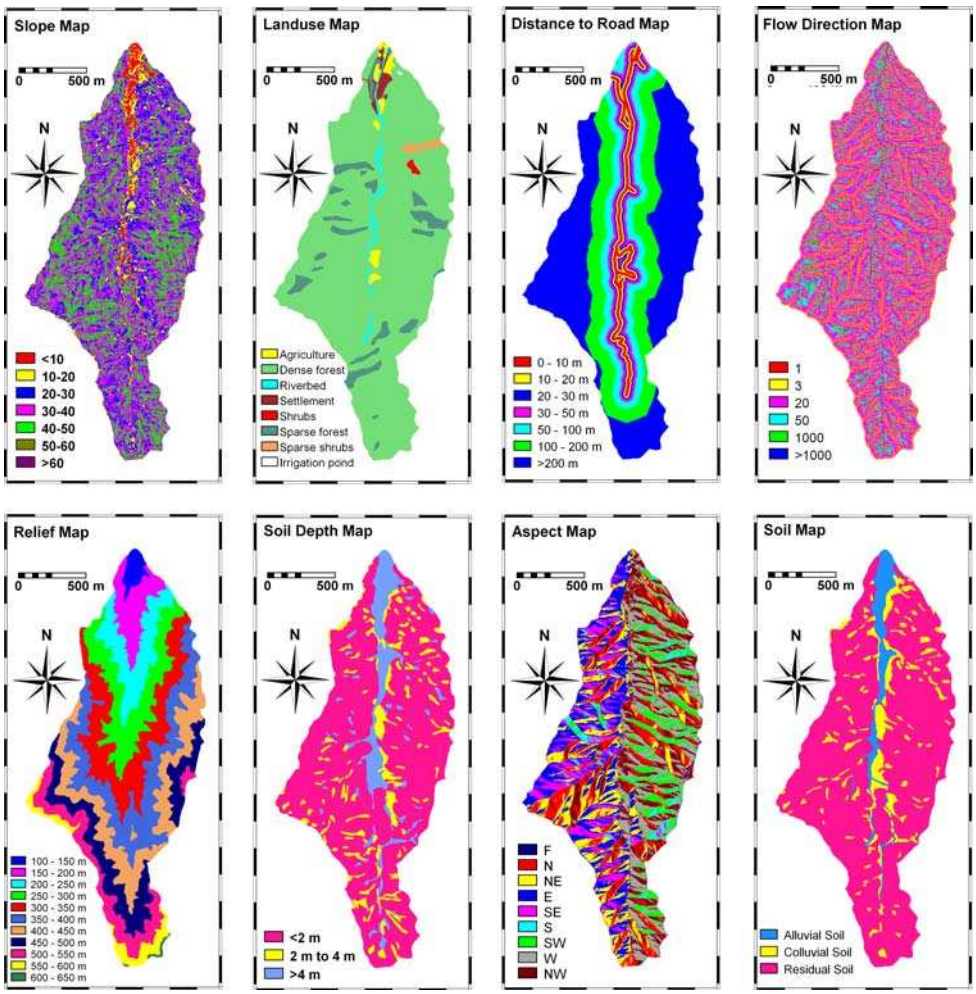

Fig. 5 Various thematic data layers prepared in GIS for the Monnyu area

slides occurs in the classes with the highest value of susceptibility maps. Effect analysis helps to validate and to check the predictive power of selected factors and classes that are used in susceptibility analysis.

Three landslide susceptibility index maps were prepared for each area and named as Main, Case A and Case B landslide susceptibility maps. Main map was prepared by adding all weight as per Eq. 5. Case A susceptibility map was prepared by adding W_fSlope, W_fFA, W_fSoil, and W_fDepth, whereas Case B map was prepared by adding W_fSlope, W_fFA, W_fSoil, W_fDepth, W_fRelief and W_fLanduse. The success rate curves of all three maps of both Moriyuki and Monnyu are shown in Fig. 6. These curves explain how well the model and factors predict landslides. To obtain the success rate curve for each LSI map, the calculated index values of all pixels in the maps were sorted in descending order. Then the ordered pixel values were categorised into 100 classes with 1% cumulative intervals. These classified maps were crossed with the landslide inventory map. Then the success rate curve was made from cross table values. In the case of Moriyuki, when all factor was used (main map), in 10% class of the study area, the LSI had a higher rank and could explain 46% of all landslides. Likewise, 30% of LSI value could explain 72% of all landslides. Similarly, in the case of Monnyu area, 15% of area where the LSI had a higher rank could explain 50% of all landslides. Figure 6 provides the percentage coverage of landslides in various higher rank percentage of LSI. With the help of this success rate curve of main map of Moriyuki, the corresponding value of LSI in 10, 30, 50 and 70% class were selected and five landslide susceptibility zones, viz very low, low, moderate, high and very high were established to prepare the classified landslide susceptibility maps after weights-of-evidence modelling (Fig. 7). Similar procedures were used for Monnyu area also, but the corresponding value of LSI in 15, 35, 55 and 75% classes were selected as per the concentration of landslide percentage. The susceptibility map of Monnyu area after weights-of-evidence modelling is given in Fig. 8.

To compare the landslide susceptibility results, the areas under the curves (Lee 2004, 2005; Lee and Talib 2005; Lee and Sambath 2006) were estimated from the rate graphs

Table 1 Computed weights for classes of various data layers based on landslide occurrences

Name of catchments	Moriyuki catchment				Monnyu catchment			
Theme class	Landslide occurences % (total landslide area is 8323 pixels)	Area % (total area of catchment is 563970 pixels)	Ratio (%Landslides/ %Area)	WFinal	Landslides occurences % (total landslide area is 10511 pixels)	Area % (total area of catchment is 345091 pixels)	Ratio (%Landslides/ %Area)	WFinal
Slope								
<10	1.54	10.39	0.15	–2.097	0.15	3.49	0.04	–3.223
20–30	4.41	15.95	0.28	–1.506	2.50	8.32	0.30	–1.316
20–30	22.84	24.24	0.94	–0.158	17.38	23.18	0.75	–0.403
30–40	44.76	31.58	1.42	0.493	40.15	38.30	1.05	0.046
40–50	23.21	15.43	1.50	0.436	33.07	23.85	1.39	0.439
50–60	3.09	2.32	1.33	0.222	6.52	2.79	2.33	0.897
>60	0.16	0.09	1.80	0.521	0.23	0.06	3.52	1.309
Slope aspect								
Flat	0.38	3.33	0.12	–2.243	0.00	0.05	0.00	–2.260[a]
North	5.26	15.68	0.34	–0.591	5.60	15.03	0.37	–0.595
Northeast	12.58	19.59	0.64	–0.573	7.22	14.36	0.50	–0.799
East	25.75	16.84	1.53	0.507	23.51	17.46	1.35	0.374
Southeast	27.20	12.28	2.21	0.962	19.77	8.76	2.26	0.974
South	13.89	8.66	1.60	0.501	8.32	2.41	3.45	1.369
Southwest	4.24	4.27	0.99	–0.046	12.82	8.69	1.47	0.438
West	5.03	6.90	0.73	–0.379	14.01	17.63	0.80	–0.293
Northwest	5.66	12.46	0.45	–0.914	8.74	15.50	0.56	–0.679
Relief								
50–100 m	0.00	4.84	0.00	–6.779[a]	–	–	–	–
100–150 m	0.26	9.65	0.03	–3.762	0.06	1.76	0.03	–3.515
150–200 m	6.69	14.08	0.48	–0.885	2.69	5.95	0.45	–0.885
200–250 m	19.10	18.42	1.04	–0.004	11.25	8.91	1.26	0.226
250–300 m	30.94	17.71	1.75	0.697	13.10	12.35	1.06	0.027
300–350 m	23.31	13.76	1.69	0.607	24.02	15.66	1.53	0.509
350–400 m	5.41	8.79	0.61	–0.579	27.13	16.94	1.60	0.582
400–450 m	4.35	6.65	0.65	–0.504	14.02	14.82	0.95	–0.109
450–500 m	6.84	4.56	1.50	0.388	6.71	11.54	0.58	–0.653
500–550 m	2.60	1.43	1.81	0.569	1.01	8.43	0.12	–2.272
550–600 m	0.50	0.11	4.47	1.505	0.00	3.37	0.00	–6.453[a]
600–650 m	–	–	–	–	0.00	0.28	0.00	–3.931[a]

Table 1 continued

Name of catchments	Moriyuki catchment				Monnyu catchment			
Theme class	Landslide occurences % (total landslide area is 8323 pixels)	Area % (total area of catchment is 563970 pixels)	Ratio (%Landslides/ %Area)	WFinal	Landslides occurences % (total landslide area is 10511 pixels)	Area % (total area of catchment is 345091 pixels)	Ratio (%Landslides/ %Area)	WFinal
Flow accumulation								
1	6.27	10.48	0.60	–0.636	9.12	14.00	0.65	–0.501
3	10.79	17.10	0.63	–0.610	11.94	18.91	0.63	–0.565
20	60.17	54.56	1.10	0.163	51.39	49.82	1.03	0.055
50	15.11	10.91	1.39	0.311	15.74	10.26	1.53	0.499
1000	6.88	5.16	1.33	0.242	10.15	5.18	1.96	0.749
>1000	0.77	1.79	0.43	–0.933	1.66	1.83	0.90	–0.115
Soil type								
Alluvial soil	1.75	18.98	0.09	–3.095	0.50	6.07	0.08	–3.539
Colluvial soil	13.01	9.36	1.39	–0.128	5.29	10.69	0.50	–1.742
Residual soil	85.23	71.66	1.19	0.330	94.21	83.25	1.13	0.248
Soil depth								
<2 m	76.17	53.66	1.42	0.626	96.41	78.35	1.23	0.414
2–4 m	21.49	27.88	0.77	–0.753	1.10	10.63	0.10	–4.021
>4 m	2.33	18.45	0.13	–2.668	2.48	11.02	0.23	–3.234
Land use								
Agriculture	0.19	5.55	0.03	–3.037	0.00	1.62	0.00	–5.391[a]
Dense forest	68.59	81.60	0.84	–0.326	78.78	87.01	0.91	–0.204
Grassland	3.30	0.25	13.09	3.199	0.00	0.04	0.00	–0.999[a]
Irrigation pond	0.00	0.12	0.00	–1.895[a]	–	–	–	–
Riverbed	0.00	1.87	0.00	–4.687[a]	0.20	1.84	0.11	–1.620[a]
Settlement	0.00	2.68	0.00	–5.055[a]	0.53	1.11	0.48	–0.345
Shrubs	0.67	0.40	1.69	0.931	0.90	0.26	3.54	1.770
Sparse forest	15.44	5.63	2.74	1.541	17.60	7.24	2.43	1.472
Sparse shrubs	11.80	1.90	6.22	2.412	1.98	0.78	2.53	1.407
Distance to roads								
0–10 m	2.82	5.18	0.55	–0.615	2.69	4.17	0.65	–0.438
10–20 m	4.23	4.34	0.97	–0.004	3.39	3.54	0.96	–0.021
20–30 m	3.65	3.83	0.95	–0.028	4.61	3.24	1.43	0.411
30–50 m	4.97	6.57	0.76	–0.277	9.11	5.63	1.62	0.569
50–100 m	13.72	13.04	1.05	0.082	14.21	13.07	1.09	0.128
100–200 m	31.88	19.95	1.60	0.664	23.31	23.91	0.97	–0.006
>200 m	38.72	47.08	0.82	–0.324	42.67	46.44	0.92	–0.128

[a] In this value landslide occurrence is 0, so arbitary 1 pixel was considered during calculation of WFinal

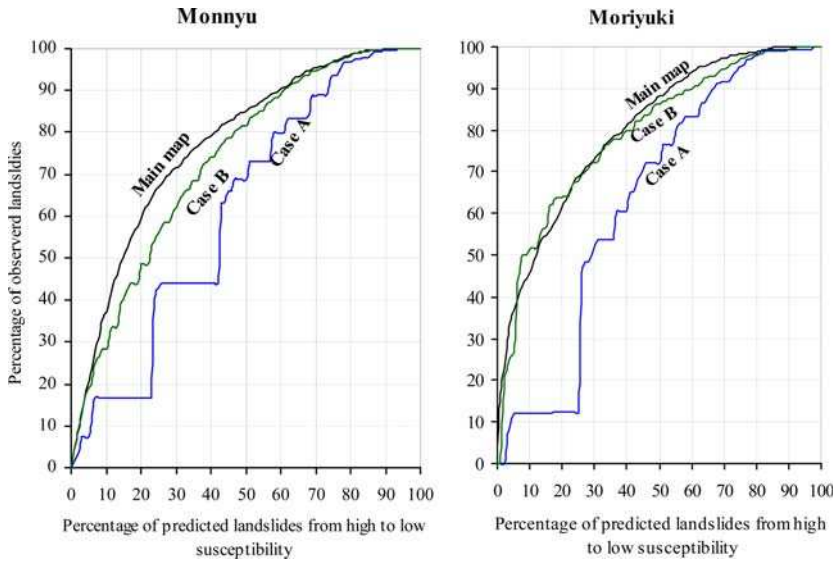

Fig. 6 Success rate curves of main susceptibility maps of Monnyu and Moriyuki and other two cases, details are given in text

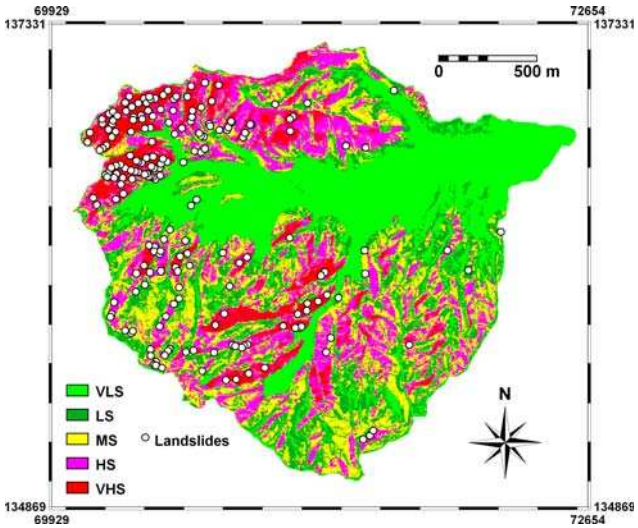

Fig. 7 Landslide susceptibility map of the Moriyuki catchment. *VHS* very high susceptibility, *HS* high susceptibility, *MS* moderate susceptibility, *LS* low susceptibility, *VLS* very low susceptibility

(see Fig. 6). A total area equal to one denotes perfect prediction accuracy for all three cases. This area under the curve qualitatively measures the prediction accuracy of the LSI value. In both catchments, it is realised that the susceptibility map prepared as per Case A is the worst case and the main map prepared after joining all the available predicting factors as per Eq. 5 is the best one. The verification demonstrates (Fig. 6; Table 2) that the main maps of both catchments show high value of area under the curve in comparison to Case A and Case B. The area under the curve of Moriyuki catchment shows a maximum of 80.7% accuracy of prediction, whereas the same of the Monnyu

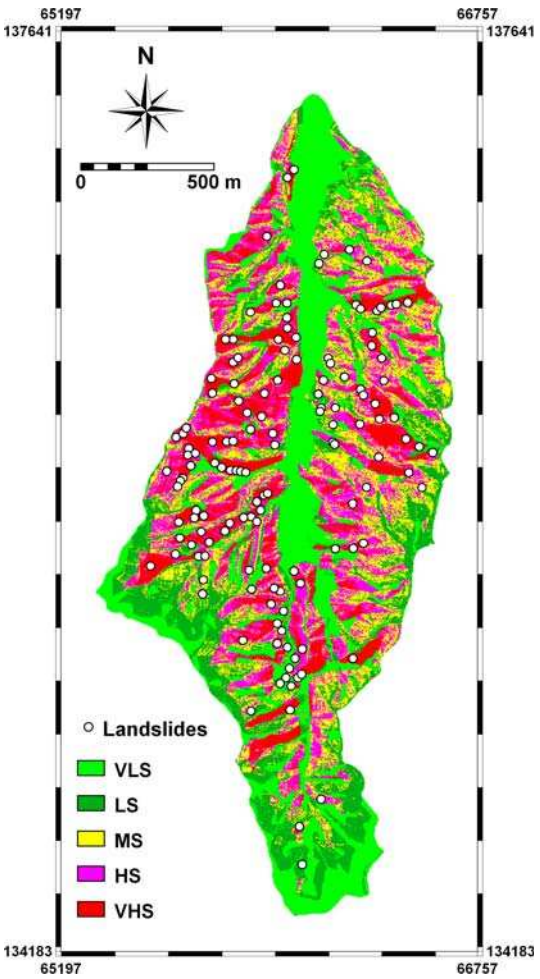

Fig. 8 Landslide susceptibility map of the Monnyu catchment. *VHS* very high susceptibility, *HS* high susceptibility, *MS* moderate susceptibility, *LS* low susceptibility, *VLS* very low susceptibility

Table 2 Area under the curve after weights-of-evidence modelling

Catchments		Main map	Case A	Case B
Moriyuki	Area under the curve	8066	6395	7972
	Ratio of the area	0.807	0.639	0.797
Monnyu	Area under the curve	7757	6192	7367
	Ratio of the area	0.776	0.619	0.737

catchment shows 77.6% accuracy. Similarly, the areas under the curve of Case B of both catchments illustrate that the selected factor parameters, slope aspect and distance to roads, have less effect in this weights-of-evidence modelling because significant increment of prediction rate could not be noticed after adding their value in the modelling (Table 2). The success rate curves of Case A of both catchments explain variable distribution of prediction. Thus, from the qualitative study of the area under the curve of success rates, it is realised that the main maps of both catchments showed satisfactory agreement between the susceptibility map and landslides location data.

Conclusions

Landslides in mountainous areas cause enormous loss of life and property every year. In such areas, landslide susceptibility mapping is very essential to delineate the landslide prone area. Various methodologies have been proposed for landslide susceptibility mappings, but in this study, the weights-of-evidence modelling with respect to bivariate statistical methods was used because data acquisition and analysis are relatively easy and less time consuming. The modelling was applied in two small catchments by considering eight predictive factors. The thematic layers of all predictive factors and existing landslides were prepared in GIS (ILWIS 3.3). Mainly DEM-based derivates and field data were used to prepare data layers of predictive factors. Both selected study areas have typical similarity in geology, soil, relief and land use. In both catchments, typhoon rainfall was the main triggering factor of landslides. As this study only deals with landslide susceptibility and not landslide hazard, information on the triggering factors of rainfall was not taken into account in this modelling. From this study, the following conclusions were made.

- A similar approach of weights-of-evidence modelling was able to predict nearly 80% of all landslides in both catchments. Thus, it could be concluded that weights-of-evidence modelling could be also useful in relatively small catchments.
- In many approaches of modelling in GIS, the model is always employed in only one area. There is very little chance of success when the approach used in that model is employed in another area. This usually happens because there is lack of similarity in the intrinsic variables at the selected sites. But, in this study, the landslide susceptibility mapping in two catchments of different area shows analogous and high success rate because of similarity in the intrinsic variables and classes. This is the reliability test of the weights-of-evidence modelling in small catchments and the results are very promising.
- This study also concludes that the approach of GIS-based modelling can give good results in the analysis of field-oriented data.
- Moreover, planning of any project at a local level requires large-scale and more accurate landslide susceptibility mapping. The attempt made in this study addresses that need to some extent. Landslide susceptibility mapping at a small catchment scale covers a lot of information that is necessary for the local level planner.

Acknowledgments We thank Mr. Toshiaki Nishimura and Mr. Eitaro Masuda for their help in the field data collection. We also acknowledge the Kagawa Prefecture Office and Ministry of Local Development Kagawa for providing aerial photographs and data. Our thanks are due to Mr. Birendra Piya, senior geologist, Department of Mines and Geology, Government of Nepal, Kathmandu for his technical assistance and comments. We would also like to thank Dr. Netra Prakash Bhandary, Ehime University, Japan for his comments on the original manuscript. Mr. Anjan Kumar Dahal and Ms. Seiko Tsuruta are sincerely acknowledged for their technical support during the preparation of this paper.

References

Agterberg FP, Bonham-Carter GF, Cheng Q, Wright DF (1993) Weights of evidence modeling and weighted logistic regression for mineral potential mapping. In: Davis JC, Herzfeld UC (eds) Computers in geology, 25 years of progress. Oxford University Press, Oxford, pp 13–32

Anbalagan D (1992) Landslide hazard evaluation and zonation mapping in mountainous terrain. Eng Geol 32:269–277

Atkinson PM, Massari R (1998) Generalized linear modelling of landslide susceptibility in the Central Apennines, Italy. Comput Geosci 24(4):373–385

Bonham-Carter GF, Agterberg FP, Wright DF (1988) Integration of geological data sets for gold exploration in Nova Scotia. Photogram Eng Remote Sens 54:1585–1592

Bonham-Carter GF, Agterberg FP, Wright DF (1989) Weights of evidence modelling: a new approach to mapping mineral potential. Stat Appl Earth Sci Geol Survey Can Paper 89–9:171–183

Bonham-Carter GF (1994) Geographic information systems for geoscientists: modelling with GIS, comp. Meth. Geos., vol. 13, Pergamon, New York, p 398

Carranza EJM, Hale M (2002) Spatial association of mineral occurrences and curvilinear geological features. Math Geol 34:203–221

Çevik E, Topal T (2003) GIS-based landslide susceptibility mapping for a problematic segment of the natural gas pipeline, Hendek (Turkey). Environ Geol 44:949–962

Cheng Q (2004) Application of weights of evidence method for assessment of flowing wells in the Greater Toronto area, Canada. Nat Resour Res 13:77–86

Chung CF, Fabbri AG (1999) Probabilistic prediction models for landslide hazard mapping. Photogram Eng Remote Sens 65(12):1389–1399

Dahal RK, Hasegawa S, Yamanaka M, Nishino K (2006) Rainfall triggered flow-like landslides: understanding from southern hills of Kathmandu, Nepal and northern Shikoku, Japan. Proceedings of the 10th international congress of IAEG, The Geological Society of London, IAEG2006 Paper number 819:1–14 (CD-ROM)

Dai FC, Lee CF, Li J, Xu ZW (2001) Assessment of landslide susceptibility on the natural terrain of Lantau Island, Hong Kong. Environ Geol 40:381–391

Daneshfar B, Benn K (2002) Spatial relationships between natural seismicity and faults, southeastern Ontario and north-central New York state. Tectonophysics 353:31–44

Emmanuel J, Carranza M, Martin Hale (2000) Geologically constrained probabilistic mapping of gold potential, Baguio district, Philippines. Nat Resour Res 9:237–253

Gökceoglu C, Aksoy H (1996) Landslide susceptibility mapping of the slopes in the residual soils of the Mengen region (Turkey) by deterministic stability analyses and image processing techniques. Eng Geol 44:147–161

Gray DH, Leiser AT (1982) Biotechnical slope protection and erosion control. Van Nostrand Reinhold, New York

Greenway DR (1987) Vegetation and slope stability. In: Anderson MG, Richards KS (eds) Slope stability. Wiley, New York, pp 187–230

Guzetti F, Carrara A, Cardinali M, Reichenbach P (1999) Landslide hazard evaluation: a review of current techniques and their application in a multi-scale study, central Italy. Geomorphology 31:181–216

Harris JR, Wilkinson L, Grunsky EC (2000) Effective use and interpretation of lithogeochemical data in regional mineral exploration programs: application of geographic information systems (GIS) technology. Ore Geol Rev 16:107–143

Hasegawa S, Saito M (1991) Natural environment, topography and geology of Shikoku, Tsushi-to-Kiso. Jpn Geotech Soc 39-9(404):19–24 (In Japanese)

Hiura H, Kaibori M, Suemine A, Yokoyama S, Murai M (2005) Sediment-related disasters generated by typhoons in 2004. In: Senneset K, Flaate K, Larsen JO (eds) Landslides and avalanches, ICFL2005, Norway, pp 157–163

Lee S, Choi J (2004) Landslide susceptibility mapping using GIS and the weight-of-evidence model. Int J Geogr Inf Sci 18:789–814

Lee S, Choi J, Min K (2002) Landslide susceptibility analysis and verification using the Bayesian probability model. Environ Geol 43:120–131

Lee S, Min K (2001) Statistical analysis of landslide susceptibility at Yongin, Korea. Environ Geol 40:1095–1113

Lee S (2004) Application of likelihood ratio and logistic regression models to landslide susceptibility mapping in GIS. Environ Manage 34(2):223–232

Lee S, Talib JA (2005) Probabilistic landslide susceptibility and factor effect analysis. Environ Geol 47:982–990

Lee S (2005) Application of logistic regression model and its validation for landslide susceptibility mapping using GIS and remote sensing data. Int J Remote Sens 26(7):1477–1491

Lee S, Sambath T (2006) Landslide susceptibility mapping in the Damrei Romel area, Cambodia using frequency ratio and logistic regression models. Environ Geol 50:847–855

Okimura T, Kawatani T (1986) Mapping of the potential surface-failure sites on granite mountain slopes. In: Gardiner V (ed) International geomorphology, Part I. Wiley, New York, pp 121–138

Pachauri AK, Gupta PV, Chander R (1998) Landslide zoning in a part of the Garhwal Himalayas. Environ Geol 36:325–334

Saha AK, Gupta RP, Sarkar I, Arora MK, Csaplovics E (2005) An approach for GIS-based statistical landslide susceptibility zonation with a case study in the Himalayas, Landslides 2:61–69

Saito M, Yuuji B, Mitsunobu F (1972) Subsurface geological map of Sanbonmatsu, northeast Kagawa (scale 1:50,000), published by Economic Planning Agency, Prefecture Office, Kagawa

Siddle HJ, Jones DB, Payne HR (1991) Development of a methodology for landslip potential mapping in the Rhondda Valley In: Chandler RJ (ed) Slope stability engineering. Thomas Telford, London pp 137–142

Soeters R, Van Westen CJ (1996) Slope instability recognition, analysis and zonation. In: Turner AK, Schuster RL (eds) Landslides, investigation and mitigation, Transportation Research Board, National Research Council, Special Report 247. National Academy Press, Washington DC, pp 129–177

Styczen ME, Morgan RPC (1995) 'Engineering properties of vegetation'. In: Morgan RPC, Rickson RJ (eds) Slope stabilisation and erosion control: a bioengineering approach. E&FN Spon, London, pp 5–58

Süzen ML, Doyuran V (2004) A comparison of the GIS based landslide susceptibility assessment methods: multivariate versus bivariate. Environ Geol 45:665–679

Tangestani MH, Moore F (2001) Porphyry copper potential mapping using the weights-of-evidence model in a GIS, northern Shahr-e-Babak, Iran. Aust J Earth Sci 48:695–701

Terlien MTJ (1996) Modelling spatial and temporal variations in rainfall-triggered landslides. PhD thesis, ITC Publ. Nr. 32, Enschede, The Netherlands, p 254

Van Westen CJ (2000) The modelling of landslide hazards using GIS. Survey Geophys 21:241–255

Van Westen CJ, Bonilla JBA (1990) Mountain hazard analysis using a PC-based GIS. In: Price DG (ed) Proceedings of the 6th international congress of IAEG, AA Balkema, Rotterdam, 1:265–271

Van Westen CJ, Rengers N, Soeters R (2003) Use of geomorphological information in indirect landslide susceptibility assessment. Nat Hazard 30:399–419

Van Westen CJ, Rengers N, Terlien MTJ, Soeters R (1997) Prediction of the occurrence of slope instability phenomena through GIS-based hazard zonation. Geol Rundsch 86:404–414

Van Westen CJ, Terlien TJ (1996) An approach towards deterministic landslide hazard analysis in GIS. A case study from Manizales (Colombia). Earth Surf Proc Landforms 21:853–868

Varnes DJ (1984) Landslide hazard zonation: a review of principles and practice, Commission on landslides of the IAEG, UNESCO, Natural Hazards No. 3, p 61

Wu W, Siddle RC (1995) A distributed slope stability model for steep forested basins. Water Resour Res 31:2097–2110

Yin KL, Yan TZ (1988) Statistical prediction model for slope instability of metamorphosed rocks. In: Proceedings of the 5th international symposium on landslides, Lausanne, 2:1269–1272

Zahiri H, Palamara DR, Flentje P, Brassington GM, Baafi E (2006) A GIS-based weights-of-evidence model for mapping cliff instabilities associated with mine subsidence. Environ Geol 51:377–386

Zêzere JL, Rodrigues ML, Reis E, Garcia R, Oliveira S, Vieira G, Ferreira AB (2004) Spatial and temporal data management for the probabilitic landslide hazard assessment considering landslide typology. In: Lacerda, Ehrlich, Fontoura and Sayâo (eds) Landslides: evaluation and stabilization, vol 1. Taylor & Fancis, London, pp 117–123